

Supplementary Information

Epitaxial growth of room-temperature ferromagnetic MnAs segments on GaAs nanowires via sequential crystallization

Joachim Hubmann,* Benedikt Bauer, Helmut S. Körner, Stephan Furthmeier, Martin Buchner, Günther Bayreuther, Florian Dirnberger, Dieter Schuh, Christian H. Back, Josef Zweck, Elisabeth Reiger, and Dominique Bougeard

Institut für Experimentelle und Angewandte Physik, Universität Regensburg, D-93040 Regensburg, Germany

E-mail: Joachim.Hubmann@ur.de

Nanowire geometry and crystalline structure under Mn supply

Figure S1(a) and S1(b) show scanning electron microscopy (SEM) images of regular, Mn-free GaAs nanowires, grown as a control experiment, and nanowires grown under (Ga,Mn)As-supply (first sample series described in the article). On both samples the wires display the same length, indicating that the supply of Mn does not inhibit the VLS growth mechanism. The only difference visible in SEM concerns the catalyst droplet: solidified Ga-droplets are perfectly spherical (Figure S1(a)), while solidified (Ga,Mn)-alloy droplets are partially faceted (Figure S1(b)). The results obtained in SEM for the second sample series described in the article (GaAs NWs with liquid Ga droplet exposed to Mn) are identical to Figure S1(b). The results obtained in SEM for the third sample series (GaAs NWs exposed to Mn

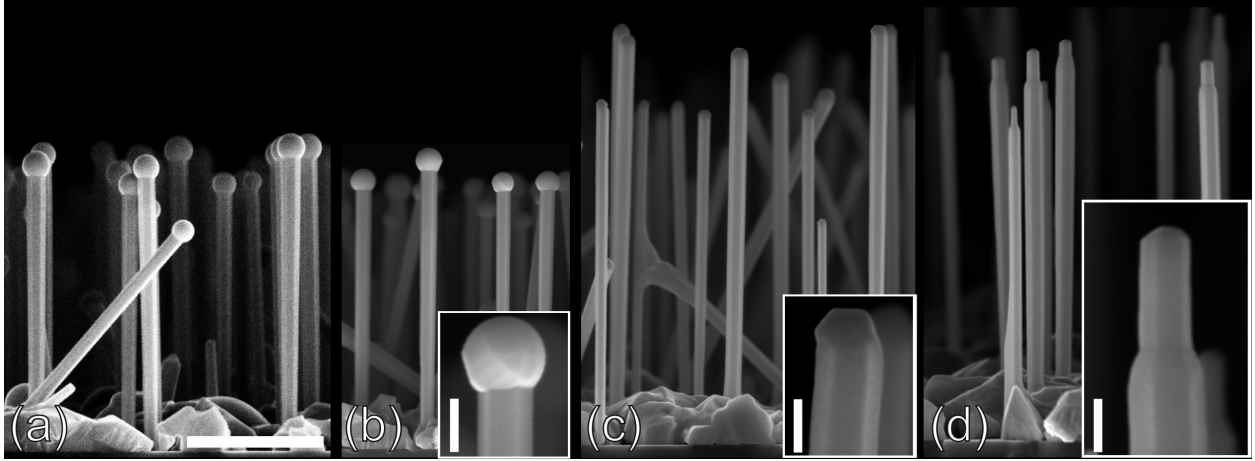


Figure S 1: Comparison of GaAs NWs and NWs grown under (Ga,Mn)As-supply: (a) standard GaAs nanowire growth with solidified Ga catalyst droplet, shown as a control experiment. (b) NWs grown under (Ga,Mn)As-supply with solidified (Ga,Mn)-alloyed droplet (first sample series described in the article). (c) NWs grown under (Ga,Mn)As-supply. The (Ga,Mn)-alloyed droplet has now been crystallized in As atmosphere, as in Figure 3 and 4 of the article. (d) GaAs NWs with crystallized Ga-droplets. These NWs have then been exposed to a Mn flux (third sample series discussed in the article). All images are normalized to the scalebar of $1 \mu\text{m}$ shown in (a). The scalebars in the insets indicate 100 nm.

in the absence of a liquid Ga droplet) are shown in Figure S1(d). Here, the GaAs NWs have been exposed to Mn, in the absence of a liquid Ga droplet, after the crystallization of the droplet under As atmosphere. The exposure to Mn does not influence the nanowire geometry, since the wires in Figure S1(d) display the typical shape of GaAs NWs and the usual tapering at the tip which is a signature of the crystallized droplet. Figure S1(c) shows an SEM image of GaAs NWs with a (Ga,Mn)-alloyed catalyst droplet which has been crystallized in As background. The crystallization of the (Ga,Mn)-alloyed droplets starts with a crystallization of pure GaAs, representing a growth continuation of the NW, and ends with the crystallization of MnAs segments of approximately 50 nm height at the tip of the NW.

Figure S1 shows that the wires obtained in all presented sample series yield the typical hexagonal side-facet orientation of GaAs nanowires without the occurrence of additional facets.

We mention in the article that we have checked wires of all sample series in TEM by scanning the wires along their entire length under HRTEM conditions. The dominant crystal structure of the NWs of all sample series is zinc-blende, with small insertions of wurtzite. A HRTEM image of a representative part of a NW grown under (Ga,Mn)As-supply (first sample series described in the article) is shown in Figure S2: By orienting the wire along $\langle 1\bar{1}0 \rangle$ zone axis, the dominant zinc-blende crystal structure is identified. The micrograph also shows two typical twin planes.

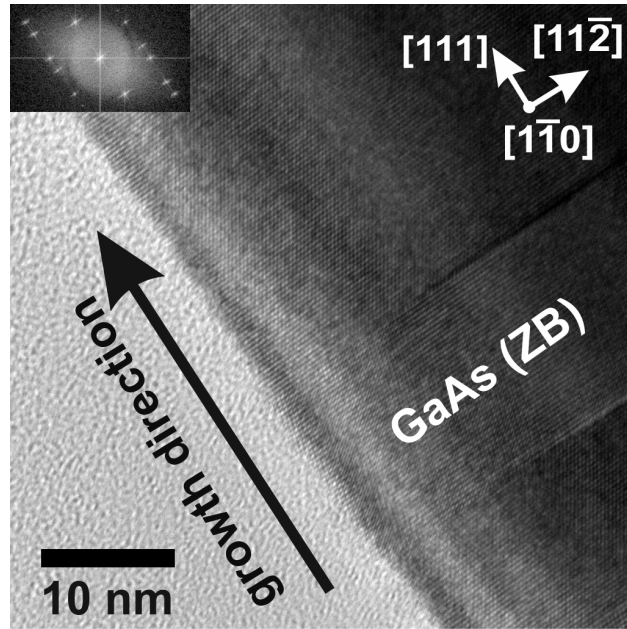


Figure S 2: HRTEM of NW grown under (Ga,Mn)As-supply (first sample series described in the article) oriented in $\langle 1\bar{1}0 \rangle$ zone axis: The main crystal structure is zinc-blende. The inset shows the corresponding fast Fourier transformation of the micrograph.

MnAs segments: Analysis of the VSM measurements

Figure S3 is an SEM image of the surface of the sample from which the NWs with MnAs segments have been removed via ultrasonication. The film-like structures which have grown between the NWs remain on the sample. As discussed in the article, this sample shows pure diamagnetism in SQUID and VSM.

Figure S4(a) shows the in-plane and out-of-plane magnetization loops of a NW ensemble

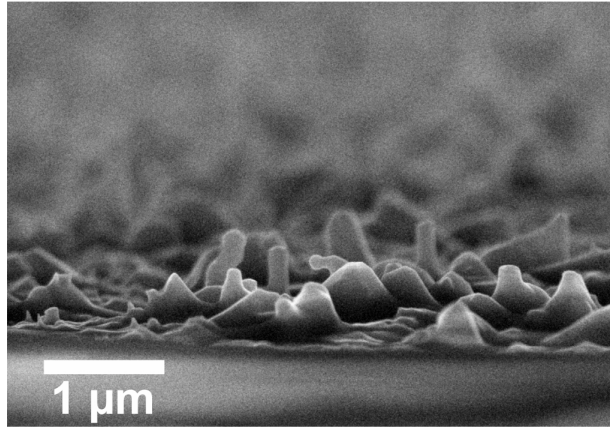


Figure S 3: SEM image of the surface of the sample from which the NWs with MnAs segments have been removed via ultrasonication. The film-like structures which have grown between the NWs remain on the sample.

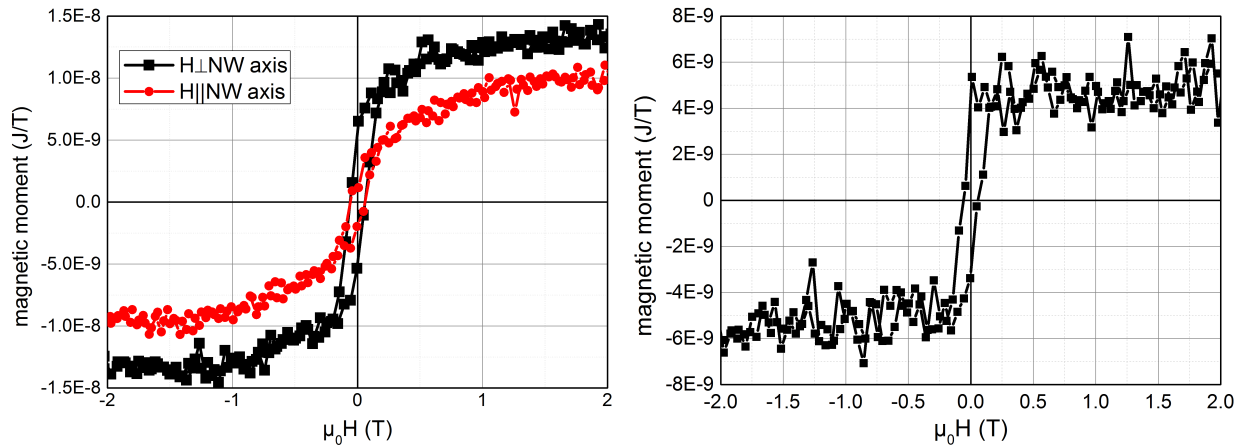


Figure S 4: Figure S4(a): In-plane and out-of-plane magnetization loops of a NW ensemble with MnAs segments at 300 K. The diamagnetic signal has been subtracted. Figure S4(b): Magnetization loop resulting from the subtraction of the out-of-plane from the in-plane measurement.

with MnAs segments at 300 K. The diamagnetic signal has been subtracted. The out-of-plane curve is subtracted from the in-plane curve, as discussed in the article, in order to obtain the magnetization loops of MnAs segments on-top of NWs which have grown perpendicular to the sample surface. The resulting magnetization loop in Figure S4(b) is characteristic for an easy axis orientation, as expected from the crystallographic relationship of the MnAs segments to the GaAs NW.

Outlook: Regrowth of GaAs on-top of the MnAs segment

For GaAs NW growth continuation on top of the MnAs segments, one possible route may be to use the scheme of Priante et al.:¹ This method requires the formation of a GaAs(111)B facet at the nanowire tip, on which a liquid Ga catalyst droplet can be formed under typical nanowire growth conditions, so that the VLS mechanism for axial nanowire growth can be initiated again. Two challenges might arise when applying this scheme to our wires terminated with MnAs segments: (i) The MnAs segment might dissolve in the deposited liquid Ga or could be unstable under the typical growth conditions around at 600°C required to continue VLS growth. (ii) GaAs growth continuation may be hampered in the absence of suitable facet orientations. As an outlook, we show in Figure S5(a) that covering the MnAs segments with low temperature (LT) GaAs protects the ferromagnetic segment, resolving point(i), and provides a basis to tune the GaAs facet orientation to address point (ii). Figure S5(a) shows a transmission electron micrograph of a GaAs nanowire on-top of which a MnAs segment has been crystallized. After covering the MnAs segment with LT GaAs ($T_{\text{Growth}} = 250^\circ\text{C}$), the wire was annealed at 600°C for 1 h to test the thermal stability of the MnAs segment. The wire was oriented in a $\langle 1\bar{1}0 \rangle$ zone axis to distinguish ZB GaAs, WZ GaAs, and WZ MnAs. The fast Fourier transform of this area (see inset) clearly reveals the coexistence of WZ MnAs and ZB GaAs. The MnAs segment induces a Moire pattern with the LT-GaAs shell that has been added. We find the same epitaxial relationship as derived in the manuscript ($[\bar{1}\bar{1}20]\text{MnAs}||[\bar{1}\bar{1}0]\text{GaAs}$, $[\bar{1}\bar{1}00]\text{MnAs}||[\bar{1}1\bar{2}]\text{GaAs}$ and $[0001]\text{MnAs}||[111]\text{GaAs}$).

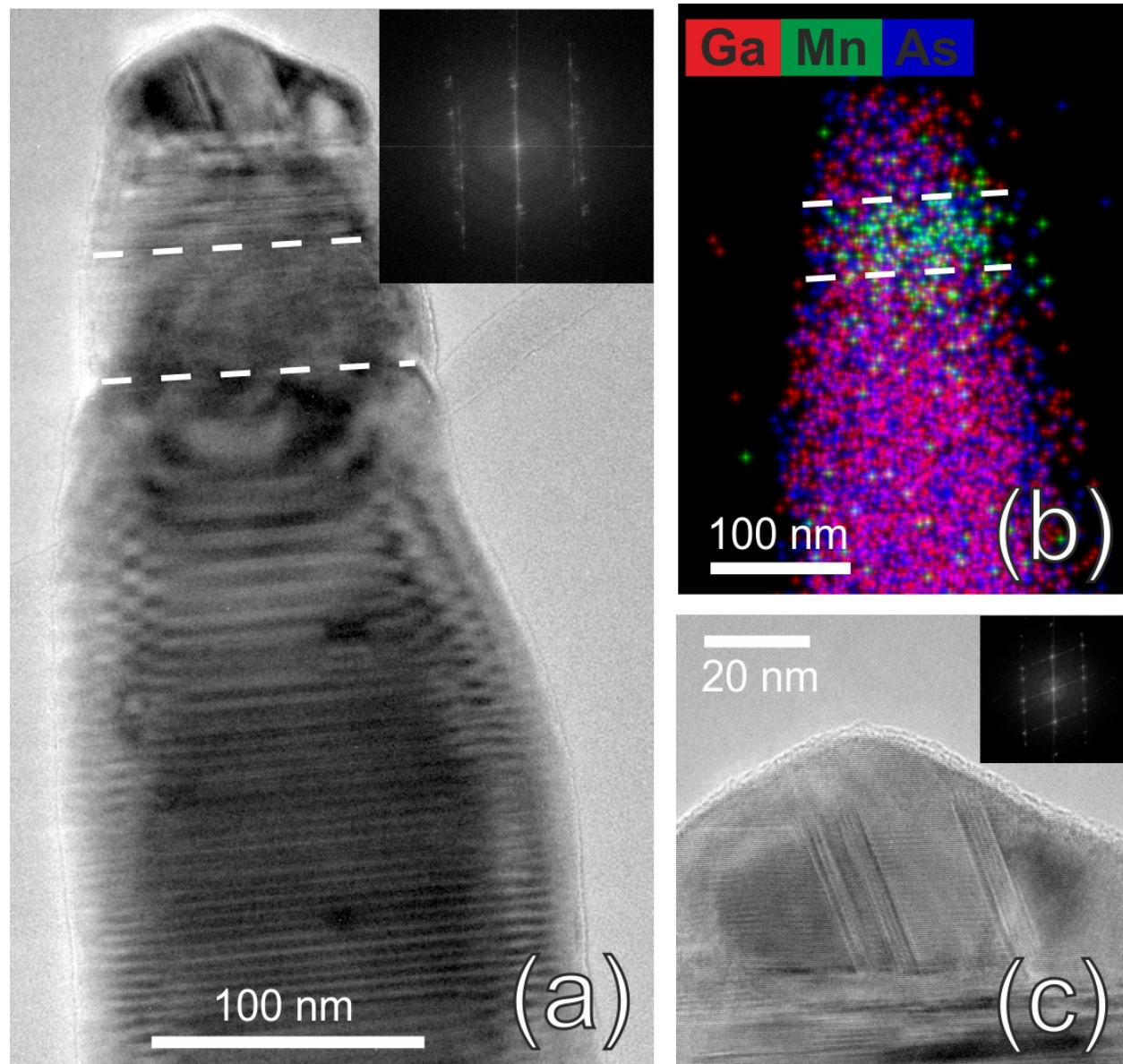


Figure S 5: (a) TEM image of a GaAs NW on top of which a MnAs segment has been crystallized and covered with low temperature (LT) GaAs. Additionally, the wire was annealed at 600°C for 1h. The MnAs segment is situated between the dashed lines, causing a Moire-pattern with the surrounding GaAs shell. The inset shows the fast Fourier transform (FFT) taken from this region only. (b) Corresponding EDX-map of this NW: The MnAs segment is covered with GaAs. (c) HRTEM of the end of the NW tip, showing the LT-GaAs: The LT-GaAs has a twinned ZB crystal structure with the same epitaxial orientation as the GaAs nanowire below the MnAs segment. The inset shows the corresponding FFT.

The MnAs segment can also be clearly identified in the EDX-image (Figure S5(b)), which corresponds to the marked area in Figure S5(a). The Figures S5(a) and S 5(b) thus demonstrate GaAs covered MnAs segments which are stable under typical VLS growth conditions. The HRTEM in Figure S5(c) shows the LT-GaAs at the end of the tip of the wire, above the MnAs segment. The crystal structure is twinned ZB, showing the same orientation as the GaAs wire below the MnAs segment. The NW is clearly terminated well defined facets. Our preliminary studies did not yield a dominant number of GaAs(111)B facets for the NW ensemble yet, indicating that further engineering of the facet orientation will be required. Possible routes are the growth of a thin GaAs shell at equilibrium conditions (typical NW growth temperatures) to shape the facets, or by the reverse reaction of GaAs nanowires,² as the GaAs(111)B facet is the least stable one occurring in GaAs nanowires.³

References

- (1) Priante, G.; Ambrosini, S.; Dubrovskii, V. G.; Franciosi, A.; Rubini, S. *Crystal Growth and Design* **2013**, *13*, 3976–3984.
- (2) Loitsch, B.; Rudolph, D.; Morkötter, S.; Döblinger, M.; Grimaldi, G.; Hanschke, L.; Matich, S.; Parzinger, E.; Wurstbauer, U.; Abstreiter, G.; Finley, J.; Koblmüller, G. *Advanced Materials* **2015**, *27*, 2125.
- (3) Millea, M. F.; Kyser, D. F. *Journal of Applied Physics* **1965**, *36*, 308–313